Reaction of the Azomethine Moiety Buried in Bilayer Membranes[1)]

Yoshio Okahata,† Reiko Ando, and Toyoki Kunitake*
Department of Organic Syntheis, Faculty of Engineering, Kyushu University, Higashi-ku, Fukuoka 812
(Received September 22, 1982)

The reaction with water and amines of the azomethine moiety that is part of single-chain ammonium amphiphiles was examined. These amphiphiles form stable bilayer aggregates when they have the alkyl tail of C_7 or C_{12}. The reaction with water of the bilayer-forming amphiphiles ceases at the hydration stage and are 10—2000 times slower than those of the amphiphiles which do not form bilayers and undergo hydrolytic cleavage. The reactivity of the azomethine moiety in bilayers decreases with increasing distance from the membrane surface. The Arrhenius plots for the bilayer-forming amphiphiles show discontinuities at temperatures corresponding to phase transition of the respective bilayer (T_c). The apparent activation energy is larger at temperatures below T_c than at temperatures above T_c. This suggests that water penetration is facilitated in the fluid bilayer. The reaction with amines was affected by their solubility in the bilayer matrix, and poly(ethylenimine) gave a much reduced reaction rate when the azomethine moiety was buried deep in the bilayer matrix.

Organic reactions in the bilayer membrane matrix are attracting increasing attention in recent years, since the highly-organized bilayer matrix offers unique media for controlling reactions. A variety of double-chain surfactants have been shown to produce stable bilayer aggregates in dilute aqueous solution.[2-5)] Physicochemical properties of these bilayer membranes are intrinsically the same as those of the biolipid bilayer and, therefore, their unique properties have been examined in relation to catalysis of some organic reactions.[6)]

We showed previously that single-chain ammonium amphiphiles which possess the *N*-benzylideneaniline moiety (C_n–BB–C_m–N^+) in the hydrophobic portion produce stable bilayer aggregates in water.[7,8)] The aggregate morphology changes extensively with the molecular structure of the amphiphile. For instance, the stable bilayer structure is apparently not formed when the length of the alkyl tail is shorter than C_7. The linear amphiphiles (C_n–BB–N^+ and C_n–BB–C_m–N^+, n=7,12) form multi-walled bilayer vesicles, whereas an amphiphile with the bent rigid segment (p-C_{12}–BB–m-C_4–N^+) gives tubular aggregates.

The variation in morphology necessarily leads to the change in the packing and/or location of the *N*-benzylideneaniline moiety in the aggregate, which, in turn, may produce changes in its reactivity.

The bilayer aggregates of C_n–BB–C_m–N^+ are stable in neutral and alkaline solution; however, they slowly decompose in acidic media due to reaction at the *N*-benzylideneaniline moiety. This group readily reacts with amine nucleophiles, and the reactivity may also depend on the aggregate morphology. We describe in this paper reactions of the azomethine moiety that is part of the bilayer structure. The relation between aggregate morphology and reactivity, once established, would give important means to control organic reactions in aqueous media.

Experimental

Syntheses of amphiphiles containing the *N*-benzylideneaniline moiety(C_n–BB–N^+, C_n–BB–C_m–N^+) and aggregation behavior of these amphiphiles have been reported elsewhere.[7,8)] Electron microscopy was performed by using a Hitachi H-500 instrument.[7)] Differential scanning calorimetry was carried out with a Daini-Seikosha SSC-560 instrument. Sample solutions(1—2 wt%, 0.02—0.05 M)(1 M=1 mol dm^{-3}) were sealed in silver pans and the thermal measurement was repeated from 3 °C to 90 °C at a rate of 2 °C/min. The detail is described elsewhere.[9)]

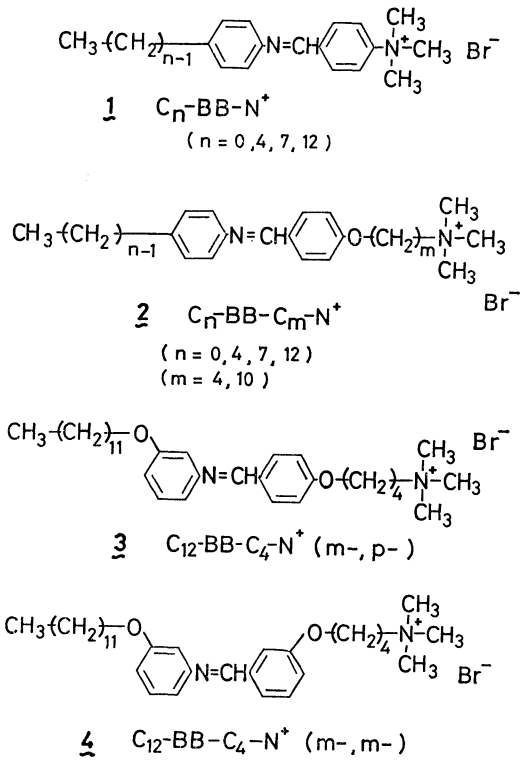

Chart 1.

Acid hydrolyses of aqueous C_n–BB–C_m–N^+ were performed usually at 30 °C, pH 5.5(0.02 M phosphate buffer) and μ=0.02(KCl). A stock solution(10^{-3}—10^{-2} M) of an amphiphile was prepared by sonication(Branson Sonifier 185) in a weakly alkaline solution(pH 9), and the reaction was initiated by adding 0.1—0.01 ml of this solution to an acidic buffer solution. The course of reaction was followed by disappearance of the absorption due to the azomethine linkage(–CH=N–) at 320 nm with a Hitachi 200 spectrophotometer. Pseudo first-order kinetics were observed up to at least 70—80% completion of the reaction, and apparent rate constants(k_{obsd}) were estimated. The pH

† Present address: Department of Polymer Science, Tokyo Institute of Technology, O-okayama, Meguro-ku, Tokyo 152.

of the reaction medium was maintained within ±0.05 during the reaction(HM-10B digital pH meter, Toa Electronics). The reaction with amines was followed in the same way.

Results

The Course of Reaction. The time course of the spectral change due to reaction of the C_{12}–BB–C_4–N^+ bilayer aggregate is shown in Fig. 1. C_{12}–BB–C_4–N^+ possesses absorption maxima at 280 nm and 320 nm. The latter peak that is attributable to the azomethine linkage[10,11] diminished with time. The absorption maximum and the spectral pattern were not influenced by the alkyl chain length (C_n and C_m). C_{12}–BB–C_4–N^+ in 50 v/v% EtOH–H_2O where the amphiphile does not form the bilayer aggregate gave the same spectral change as that of Fig. 1. It means that the spectra of C_n–BB–C_m–N^+ and C_n–BB–N^+ are not affected by the aggregate formation. Therefore, the spectrum of the amphiphile and the course of reaction are concluded to be identical irrespectively of the bilayer formation.

Acid hydrolysis of the azomethine linkage is initiated by proton addition to nitrogen followed by the rate-limiting nucleophilic attack of H_2O or OH^-, as shown in Eq. 1.[12] It is assumed that the same mechanism operates in the aqueous micelle[13] and in liquid crystalline media.[14]

$$\text{-CH=N-} \underset{\text{fast}}{\overset{H^+}{\rightleftharpoons}} \text{-CH=}\overset{+}{\text{N}}\text{H-} \underset{\text{slow}}{\overset{H_2O}{\rightleftharpoons}} \text{-CH(OH)-NH-} \rightleftharpoons$$

$$\text{-CH(O}^-\text{)-}\overset{+}{\text{N}}\text{H}_2\text{-} \rightleftharpoons \text{-CHO} + \text{H}_2\text{N-} \qquad (1)$$

Disappearance of the azomethine absorption at 320 nm that is used for following the reaction does not assure completion of Eq. 1. In the case of BB–N^+ and C_4–BB–C_4–N^+ which do not form bilayers, thin-layer chromatography of the reaction mixture indicated formation of the corresponding amines and aldehydes, and therefore, the reaction proceeds to completion according to Eq. 1. On the other hand, in the bilayer system, the reaction appears to stop at the hydration step from the following reasons: (1) The bilayer structure remains in electron micrographs after the reaction, as discussed below (Fig. 4b); (2) equimolar mixtures of the product amines and aldehydes do not give clear solution under the same conditions, although the reaction mixture remains clear after the reaction is over; (3) when the homogeneous reaction mixture is mixed with concentrated hydrochloric acid and refluxed, the product amine and aldehyde separate as white precipitates. Therefore, the reaction stops at the intermediate stage without the acid treatment. For these reasons, hydrolysis and hydration will not be discriminated in the subsequent discussion as long as the kinetics are concerned.

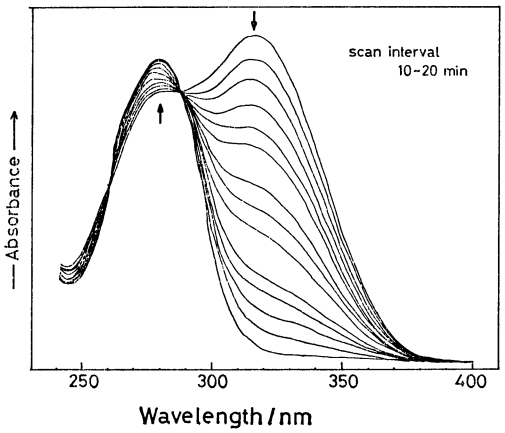

Fig. 1. Spectral change due to reaction of aqueous C_{12}–BB–C_4–N^+ bilayer.
30 °C, pH 3.4 (0.02 M acetate buffer), μ=0.02 (KCl), [C_{12}–BB–C_4–N^+]=1.0×10^{-4} M.

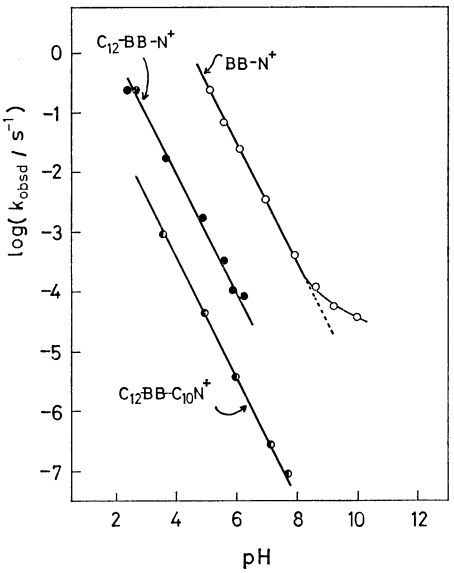

Fig. 2. pH-rate profiles of the reaction of C_n–BB–C_m–N^+.
30 °C, 0.02 M acetate buffer (pH 2—5), 0.02 M phosphate buffer (pH 6—7), 0.02 M borate buffer (pH 7—9), μ=0.02 (KCl), [C_{12}–BB–C_{10}–N^+]=6.0×10^{-5} M, [C_{12}–BB–N^+]=6.0×10^{-5} M, [BB–N^+]=6.0×10^{-4} M.

The pH-rate profile of the azomethine reaction was examined at pH 2 to 10 and those of BB–N^+, C_{12}–BB–N^+, and C_{12}–BB–C_{10}–N^+ are shown in Fig. 2 as typical examples. In all cases, log k_{obsd} decreases linearly with the slope of −1 at pH 2 to 8. This is consistent with the above-mentioned supposition that the reaction proceeds *via* the specific acid catalysis (Eq. 1). The upward curvature for BB–N^+ at pH 8—10 indicates the involvement of water or hydroxide catalysis. The catalytic effect of the basic buffer species (HBO_3^-, HPO_4^-, and $CH_3CO_2^-$) was negligibly small and the effective nucleophilic species is limited to water at buffer concentrations of 0.005 to 0.02 M. The subsequent experiments were conducted at pH 5.5 because of the experimental convenience.

Electron Microscopy. It is expected that the reaction alters the aggregate morphology drastically. An electron micrograph for an aqueous solution of C_{12}–BB–C_4–N^+ (5×10^{-3} M) is shown in Fig. 3a, which indicates the presence of multi-walled vesicles. A reacted sample for electron microscopy was obtained as follows: One ml of the same aqueous solution as that

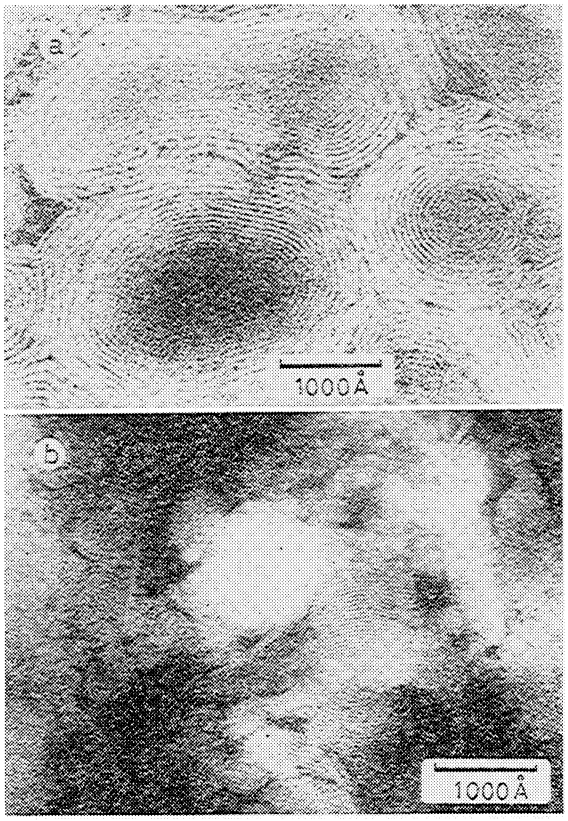

Fig. 3. Electron micrographs before (a) and after (b) reaction of C_{12}–BB–C_4–N^+ aggregates with water. Initial magnification, ×50,000, stained by uranyl acetate.

used for the rate measurement was adjusted to pH 1—2 by adding one drop of concentrated hydrochloric acid, and maintained at room temperature for 1 h. Complete disappearance of the absorption at 320 nm was confirmed, and the solution was stained with aqueous uranyl acetate (1 wt%). An electron micrograph for this sample is shown in Fig. 3b. The lamellar structure is preserved even after complete disappearance of the azomethine linkage.

As mentioned above, the acid-catalyzed reaction supposedly ceases to proceed at the hydration step of Eq. 1. The bilayer assemblage of the hydrated intermediate may suppress the subsequent cleavage step. It is interesting to note that the hydrogenation product of this amphiphile, **5**, gives tubular aggregates, in contrast to formation of lamellar aggregates by the hydration product.

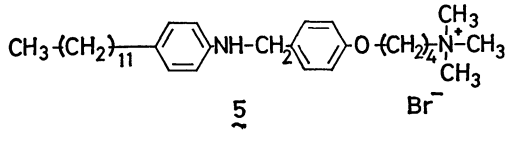

5

Chart 2.

Amphiphile Structure and Reaction Rate. Figure 4 illustrates the dependence of the reaction rate on the amphiphile concentration. In Fig. 4a is given the concentration dependence for three amphiphiles whose total alkyl lengths (C_n+C_m) are 10 to 12. They react more slowly than BB–N^+ which does not have the

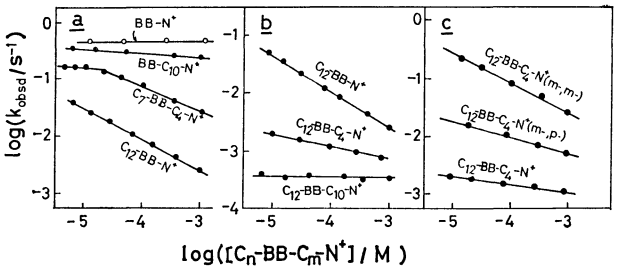

Fig. 4. Concentration dependence of the rate constant. 30 °C, pH 5.5±0.1 (0.02 M phosphate buffer), μ= 0.02 (KCl).

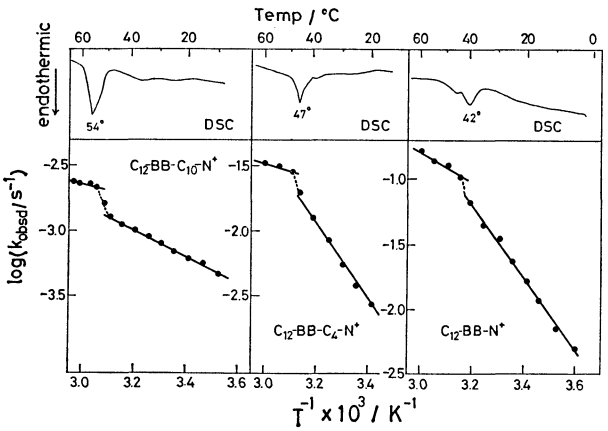

Fig. 5. Arrhenius plots of the reaction and DSC curves of C_{12}–BB–C_m–N^+ bilayers.
Reaction conditions: pH 4.3 (0.02 M acetate buffer), 0.02 M KCl, [C_{12}–BB–C_m–N^+]=6.1×10^{-5} M DSC samples: [C_{12}–BB–C_m–N^+]=1—2 wt% (2—5×10^{-2} M).

alkyl chain. It is interesting that the reaction rate varies considerably among the three amphiphiles in spite of their closely-related structures (only the distribution of the alkyl chain is different). The reaction rate is suppressed when the alkyl chain is localized in the tail portion (C_{12}–BB–N^+), but it is not so when the alkyl chain is localized in the spacer portion (BB–C_{10}–N^+). Figure 4b compares $\log k_{obsd}$ for C_{12}BB–C_m–N^+ in which the spacer length is varied. The rate as well as concentration dependence become smaller as the spacer is lengthened. The influence of the pattern of alkyl substitution at the rigid segment is shown in Fig. 4c. The meta substitution makes these amphiphiles more vulnerable to reaction than the para substitution.

Effect of Temperature. Reactions of aqueous bilayers of C_{12}–BB–C_m–N^+ (m=0, 4, 10) were performed at 0—60 °C. The corresponding Arrhenius plots are shown in Fig. 5. The three Arrhenius plots are made of two linear portions. The inflection regions are 40—45 °C, 45—50 °C, and 50—55 °C for C_{12}–BB–C_m–N^+ (m=0, 4, and 10), respectively. These temperature regions agree very closely to the endothermic region observed in the DSC measurement. The endothermic peaks are derived from the crystal-to-liquid crystal phase transition of the bilayer membrane.[7] Thus, the anomaly in the Arrhenius plots reflects the change

in the membrane physical state. In agreement with this supposition, aqueous BB–C_{10}–N^+ which does not form the bilayer structure and correspondingly gives no DSC peak gave linear Arrhenius plots.

Effect of Reaction Media. The reaction of C_{12}–BB–C_m–N^+ (m=0, 4, and 10) was examined in the bilayer matrix of dihexadecyldimethylammonium bromide ($2C_{16}N^+2C_1$), in the aqueous hexadecyltrimethylammonium bromide (CTAB) micelle, and in 50 v/v% EtOH–H_2O. The results are summarized in Table 1, in comparison with those of the single-component bilayer membrane. The k_{obsd} value decreased with increasing spacer lengths, when C_{12}–BB–C_m–N^+ were allowed to react as single-component bilayer membranes, in the $2C_{16}N^+2C_1$ bilayer or in the CTAB micelle. In contrast, the influence of the spacer length cannot be seen in the reaction in 50 v/v% EtOH–H_2O, and the k_{obsd} value is much larger in this medium than in other media. C_{12}–BB–C_m–N^+ would be molecularly dispersed in 50 v/v% EtOH–H_2O, and the azomethine moiety should be equally exposed to acid in spite of different spacer lengths, leading to the lack of the spacer effect. The observed influence of the spacer length in the other three media clearly indicates that C_{12}–BB–C_m–N^+ molecules are more or less organized in these media.

Table 1. Reaction of C_{12}–BB–C_m–N^+ (m=0, 4, and 10) in various microenvironments[a)]

Medium	$10^4 \times k_{obsd}/s^{-1}$		
	C_0	C_4	C_{10}
Water	220	44	1.3
Aqueous $2C_{16}N^+2C_1$ bilayer	120	23	1.0
Aqueous CTAB micelle	480	100	8.2
50 v/v% EtOH–H_2O	1200	1400	1300

a) 30 °C, pH 5.5 (0.02 M phosphate buffer) μ=0.02 (KCl) [C_{12}-BB-C_m-N^+]=1.0×10^{-4}, [CTAB]=1.0×10^{-3} M, [$2C_{16}N^+2C_1$]=1.0×10^{-3} M.

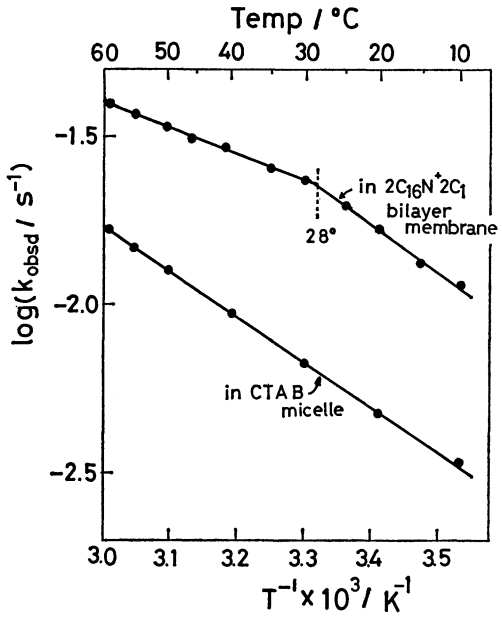

Fig. 6. Arrhenius plots of the reaction of C_{12}–BB–C_{10}–N^+ in the CTAB micelle and in the $2C_{16}N^+2C_1$ bilayer. 30 °C, pH 2.2, 0.02 M KCl, [C_{12}–BB–C_{10}–N^+]=6.0×10^{-5} M, [CTAB]=[$2C_{16}N^+2C_1$]=1.0×10^{-3} M.

Reaction with Amines. Primary amines readily undergo the exchange reaction with Schiff bases. The exchange reaction with the azomethine moiety of aqueous C_{12}–BB–C_m–N^+ (m=0, 4, and 10) was examined in the presence of excess amines. The results are summarized in Fig. 7. The overall rate (k_{all} term) of disappearance of the azomethine moiety was corrected for the water reaction in the absence of amines (k_{obsd} term). Poly (ethylenimine) used is commercially available (MW 60000) and contains 25% primary, 50% secondary, and 25% tertiary amino groups.[15)]

The rate constant increases linearly with the amine concentration, indicating occurrence of clean second-order reaction. The spacer length exerts relatively small influences in the reaction with benzylamine. The spacer effect is more apparent with dodecylamine as attacking nucleophile, although the reaction rates are smaller. In the case of poly(ethylenimine), the reactivities of C_{12}–BB–C_m–N^+ (m=4 and 10) are much smaller than that of C_{12}–BB–C_m–N^+ (m=0).

Discussion

Mode of Aggregation and Reactivity. The aggregation behavior of single-chain amphiphiles has been shown to be determined by five structural elements.[8)] They are (1) flexible tail, (2) rigid segment, (3) hydrophilic head group, (4) spacer group, and (5) additional interacting group. In the case of the amphiphiles used in this study, three structural elements (length of flexible tail, spacer length and the mode of substitution at the rigid segment) are responsible for the change in the aggregation behavior.

The rate constants(k_{obsd}) at the amphiphile concentration of 1.0×10^{-4} M are summarized in Table 2, together with the aggregation behavior. The predom-

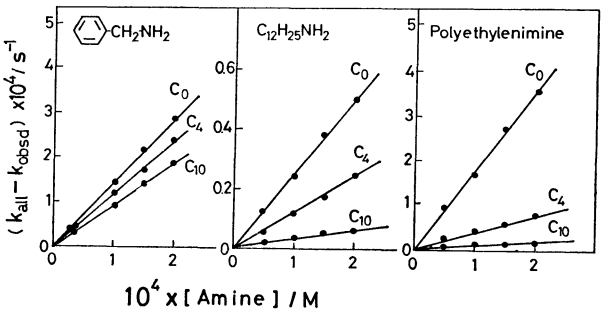

Fig. 7. Reaction of amines with C_{12}–BB–C_m–N^+ bilayers.
30 °C, pH 6.0 (0.02 M phosphate buffer), 0.02 M KCl, [C_{12}–BB–C_m–N^+]=1.0×10^{-3} M, [amine]=1.0×10^{-2} M. Unit mole is used for the polymer.

Table 2. Aggregation behavior and reactivity of C_n-BB-C_m-N^+ in water

Amphiphile	$10^3 \times$ CMC / M	Aggregate weight ($\times 10^{-4}$ dalton)	Electron micrograph	$10^4 \times k_{obsd}$[b] / s^{-1}
C_{12}-BB-C_{10}-N^+	0.01	1000	Vesicle and lamella	1.2
C_{12}-BB-C_4-N^+	0.01	400	Vesicle	44
C_{12}-BB-N^+	0.01	400	Multi-walled vesicle	220
C_7-BB-C_{10}-N^+	0.02	2000	Vesicle	7.4
C_7-BB-C_4-N^+	0.01	2000	Finger-print like	620
C_7-BB-N^+	0.06	800	Finger-print like	1000
C_4-BB-C_{10}-N^+	0.33	600	No structure	2500
C_4-BB-C_4-N^+	0.16	800	No structure	1800
C_4-BB-N^+	0.22	10	No structure	4800
BB-C_{10}-N^+	>10	400	No structure	2500
BB-N^+	>10	<1	No structure	4500
C_{12}-BB-C_4-N^+(*m*-, *p*-)	0.01	60	Rod	92
C_{12}-BB-C_4-N^+(*m*-, *m*-)	0.01	70	Pre-rod and partial lamella	450

a) Aggregation behaviors are mostly quoted from Refs. 8 and 9. b) 30 °C, pH 5.5±0.1, μ=0.02(KCl), [C_n-BB-C_m-N^+] = 1.0×10^{-4} M.

inant factors which govern the reaction rate are (1) the extent of bilayer assemblage as determined by the tail length and the pattern of substitution at the rigid segment, and (2) the distance of the reacting group from the membrane surface as determined by the spacer length. The bilayer structure is not developed for the azomethine amphiphiles with alkyl tails shorter than C_7. These amphiphiles give largest k_{obsd} values (0.2—0.5 s^{-1}). It is noteworthy that C_4-BB-C_m-N^+ (m=4 and 10) and BB-C_{10}-N^+ are among the most reactive amphiphiles in spite of their extensive aggregation (though bilayer is not formed). This means that simple aggregation without amphiphile orientation do not lead to rate suppression. Comparisons shown in Figs. 4a and 4c also point to the same conclusion. Three amphiphiles (BB-C_{10}-N^+, C_7-BB-C_4-N^+ and C_{12}-BB-N^+) of Fig. 4a possess similar amounts of the alkyl chain and form equally huge aggregates (aggregate weight, 4—20 millions). However, their reactivities change drastically due to varying extents of orientation. The reactivities of amphiphiles with different patterns of substitution are compared in Fig. 4c. The molecular orientation in the aggregate as examined by electron microscopy becomes less ordered, as the meta substitution increases. The reaction rate becomes greater accordingly.

The influence of the distance of the reacting group from the membrane surface is found in Table 2 for several combinations. In the series of C_{12}-BB-C_m-N^+ (m=0, 4, and 10) which all give fully developed bilayers, the reaction rate decreases as the spacer becomes longer (see also Fig. 4b). The same trend is found for a series of less developed bilayers: C_7-BB-C_m-N^+ (m=0, 4, and 10). The spacer effect is similarly noticed when amphiphiles C_{12}-BB-C_m-N^+ are buried in the $2C_{16}N^+2C_1$ bilayer matrix and in the CTAB micelle (Table 1), but it totally disappears in 50 v/v% EtOH-H_2O. The ordered structure may persist in the CTAB micelle.

Additional examples of the spacer effect are obtained for Schiff-base exchange reaction of the azomethine bilayer with amines. As shown in Fig. 7, the reaction rate decreases with increasing spacer lengths, and the extent of the spacer effect (rate difference) varies with the structure of amines. Benzylamine produces the smallest spacer effect and the rate difference is largest for poly(ethylenimine). Benzylamine should be incorporated into the bilayer matrix relatively nonspecifically; hence, small spacer effects. Dodecylamine is expected to align better in the membrane matrix. This factor would lead to larger differences in relative rate. Poly(ethylenimine) is highly water-soluble, and would not readily penetrate into the bilayer matrix. In consistence with this supposition, the azomethine moiety near the membrane surface (no spacer) reacts much faster with the polymer than those buried in the membrane (spacer: C_4 and C_{10}).

As for the reactant orientation in the bilayer matrix, Czarniecki and Breslow examined the photosensitized hydrogen abstraction by benzophenones in the dihexadecyl phosphate bilayer.[16] They showed the bilayer lamella produced better orientation of the reagents than the bilayer vesicle, although the difference was not remarkable.

Membrane Physical State and Reactivity. The Arrhenius plots of the azomethine reaction show discontinuity near the phase transition of the respective membrane (Fig. 5). When the reaction was carried out in the $2C_{16}N^+2C_1$ bilayer, an inflection in the Arrhenius plots was found at T_c of the matrix membrane (Fig. 6). No inflection was observed in the CTAB micelle. Figure 8 is schematic illustrations of the membrane physical state. The component molecules are highly aligned and the molecular movement is suppressed in the gel(crystalline) state. However, the alignment becomes less ordered and the alkyl chain can assume multiple conformations in the liquid-crystalline state, although the bilayer structure is maintained. This change in the membrane physical state could produce the reactivity difference, and discontinuities observed in the Arrhenius plots (Fig. 5) may be related to coexistence of the two physical states during phase transition.

Table 3 summarizes the apparent activation energy

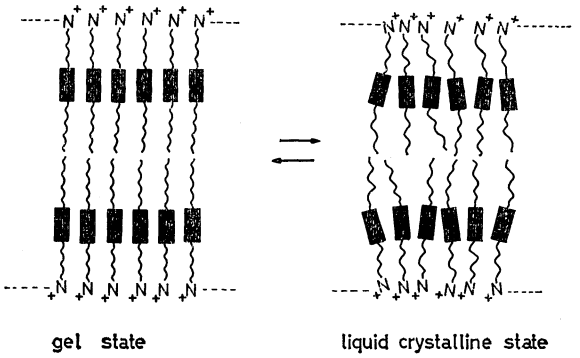

Fig. 8. Schematic illustrations of the phase transition of the C_n–BB–C_m–N^+ bilayer membrane.

Table 3. Apparent activation energy of the reaction of C_{12}–BB–C_m–N^+ aggregates

Aggregate	E_a/kJ mol^{-1}		ΔE_a
	Below T_c	Above T_c	
C_{12}–BB–N^+ bilayer	67	20	56
C_{12}–BB–C_4–N^+ bilayer	54	11	45
C_{12}–BB–C_{10}–N^+ bilayer	19	7.5	12
C_{12}–BB–C_{10}–N^+ in $2C_{16}N^+2C_1$ bilayer	16	12	4.2
C_{12}–BB–C_{10}–N^+ in CTAB micelle	(13)		—

E_a of the reaction. In all the three single-component bilayers, the activation energy is greater in the temperature region below T_c than above T_c. This is not unexpected results, since the azomethine reactivity would certainly be suppressed in the rigid membrane matrix. In several reactions where reactants are buried in the membrane matrix, the activation energy increased in the temperature below T_c. For example, E_a was 167 and 84 kJ/mol at temperatures below and above T_c, respectively, in the case of proton abstraction of Eq. 2.[17] Nucleophilic displacement of a phosphate ester by hydroxamates (Eq. 3) gave similar E_a difference (88 and 59 kJ/mol)[18]

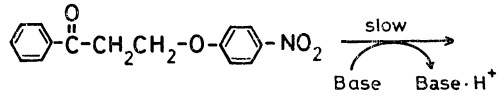

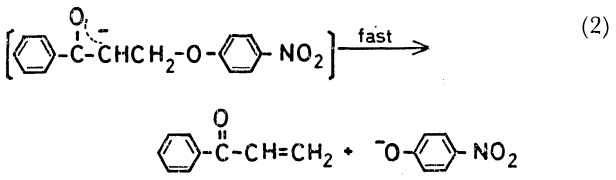

(2)

In the present system, the E_a values observed at temperatures above T_c are small and, correspondingly, its variation among different bilayers (C_{12}–BB–C_m–N^+, m=0, 4, and 10) is small. The E difference is much greater at temperatures below T_c. In both cases, E_a values become smaller as the spacer length is increased, and the E_a difference due to phase transition (ΔE_a) is 58 kJ/mol for the C_{12}–BB–N^+ bilayer and is only 12 kJ/mol for the C_{12}–BB–C_{10}–N^+ bilayer. It has been pointed out that longer spacers lead to stabilization of the bilayer structure.[8] The rate constant of the azomethine reaction decreases with the spacer length (Table 1). Thus, it is suggested that the temperature dependence is diminished for well-developed bilayers or when the reacting moiety is buried deep in the matrix. Interestingly, the concentration dependence of the reaction rate shows a pattern (Fig. 4b) analogous to that of the temperature effect in that the reaction of the C_{12}–BB–C_{10}–N^+ bilayer gives a much reduced concentration dependence relative to that of the C_{12}–BB–N^+ bilayer.

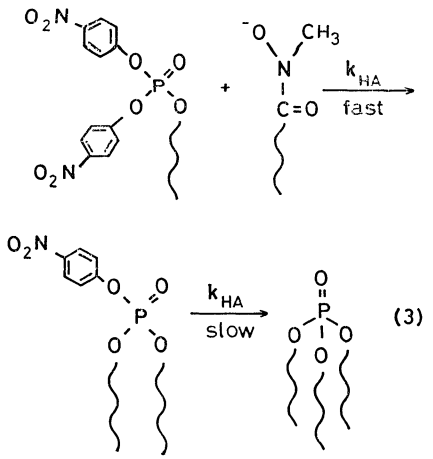

(3)

When C_{12}–BB–C_{10}–N^+ is buried in the $2C_{16}N^+2C_1$ matrix, the reactivity is much enhanced and an inflection in the Arrhenius plots is observed near T_c of the matrix membrane. The enhanced reactivity suggests that the cluster formation of C_{12}–BB–C_{10}–N^+, if present, is not significant. The inflection observed at T_c of the matrix membrane, not at T_c of the substrate itself, is not inconsistent with the cluster formation.

Conclusion

It is established in this investigation that the reactivity of a functional group is governed by molecular orientation (bilayer formation) in the aggregate, and if bilayer is formed, by distance from the membrane surface and membrane physical state. These results would provide valuable information on peculiar reactivities associated with bilayer characteristics.

References

1) Contribution No. 670 from the Department of Organic Synthesis.

2) T. Kunitake and Y. Okahata, *J. Am. Chem. Soc.*, **99**, 3860 (1977); *Chem. Lett.*, **1977**, 1337; T. Kunitake, Y. Okahata, K. Tamaki, F. Kumamaru, and M. Takayanagi, *ibid.*, **1977**, 387.

3) T. Kunitake and Y. Okahata, *Bull. Chem. Soc. Jpn.*, **51**, 1877 (1978).

4) Y. Okahata, S. Tanamachi, M. Nagai, and T. Kunitake, *J. Colloid Interface Sci.*, **82**, 401 (1981).

5) For reviews; T. Kunitake, *J. Macromol. Sci. Chem.*, **A13**, 587 (1979); J. H. Fendler, *Acc. Chem. Res.*, **13**, 7 (1980).

6) For a review, T. Kunitake and S. Shinkai, *Adv. Phys. Org. Chem.*, **17**, 435 (1980).
7) T. Kunitake and Y. Okahata, *J. Am. Chem. Soc.*, **102**, 549 (1980).
8) T. Kunitake, Y. Okahata, M. Shimomura, S. Yasunami, and K. Takarabe, *J. Am. Chem. Soc.*, **103**, 5401 (1981).
9) Y. Okahata, R. Ando, and T. Kunitake, *Ber. Bunsenges. Phys. Chem.* **85**, 789 (1981).
10) E. H. Cordes and W. P. Jencks, *J. Am. Chem. Soc.*, **84**, 832 (1962).
11) R. L. Reeves, *J. Am. Chem. Soc.*, **84**, 3332 (1962).
12) W. P. Jencks, "Catalysis in Chemistry and Enzymology," McGraw-Hill, New York, N. Y. (1969), Chap. 3.
13) M. T. A. Behme and E. H. Cordes, *J. Am. Chem. Soc.*, **87**, 260 (1965).
14) W. E. Bacon, *Mol. Cryst. Liq. Cryst.*, **67**, 101 (1981).
15) L. E. Davis, "Water-soluble Resins," ed by R. L. Davidson and M. Sittig, Reinhold Publ. New York, (1968), p. 1216; G. M. Lukovkin, V. S. Pshezhetsky, and G. A. Murtazaeva, *Eur. Polym. J.*, **9**, 559 (1973).
16) M. F. Czarniecki and R. Breslow, *J. Am. Chem. Soc.*, **101**, 3675 (1979).
17) Y. Okahata, S. Tanamachi, and T. Kunitake, *Nippon Kagaku Kaishi*, **1980**, 442.
18) Y. Okahata, H. Ihara, and T. Kunitake, *Bull. Chem. Soc. Jpn.*, **54**, 2072 (1981).
19) Y. Okahata, H. Ihara, and T. Kunitake, *J. Am. Chem. Soc.*, submitted.